
A Review of Factors That Affect Artifact From Metallic Hardware on Multi-Row Detector Computed Tomography

Milliam L. Kataoka, MD,^a Mary G. Hochman, MD,^a Edward K. Rodriguez, MD,^b Pei-Jan Paul Lin, PhD,^a Shigeto Kubo, MD,^a and Vassilios D. Raptopoulos, MD^a

Artifact arising from metallic hardware can present a major obstacle to computed tomographic imaging of bone and soft tissue and can preclude its use for answering a variety of important clinical questions. The advent of multirow detector computed tomography offers new opportunities to address the challenge of imaging in the presence of metallic hardware. This pictorial essay highlights current strategies for reducing metallic hardware artifacts and presents some illustrative clinical cases.

Artifact arising from metallic hardware can degrade computed tomographic (CT) images, limiting their clinical utility. The advent of multirow detector computed tomography (MDCT) provides new opportunities to address the challenge of artifact from orthopedic or other metallic hardware.¹⁻³ Metal artifacts appear as a streaking effect on an image, with areas of increased and decreased density obscuring adjacent structures (Fig 1). These artifacts occur because metal hardware causes beam hardening and severely attenuates the X-ray beam, resulting in incomplete projection data and subsequent reconstruction artifacts.^{4,5} (Fig 2). This pictorial essay reviews current strategies for reducing metallic artifacts.

Materials and Methods

Two phantoms were constructed using a ham bone and surrounding musculature, fitted with a buttress plate

From the Department of ^aRadiology and ^bOrthopedics Beth Israel Deaconess Medical Center, Boston, MA.

Reprint requests: Mary G. Hochman, MD, Department of Radiology, Beth Israel Deaconess Medical Center, 330 Brookline Avenue, Boston, MA 02215. E-mail: mhochman@bidmc.harvard.edu.

Curr Probl Diagn Radiol 2010;39:125-136.

© 2010 Mosby, Inc. All rights reserved.

0363-0188/\$36.00 + 0

doi:10.1067/j.cpradiol.2009.05.002

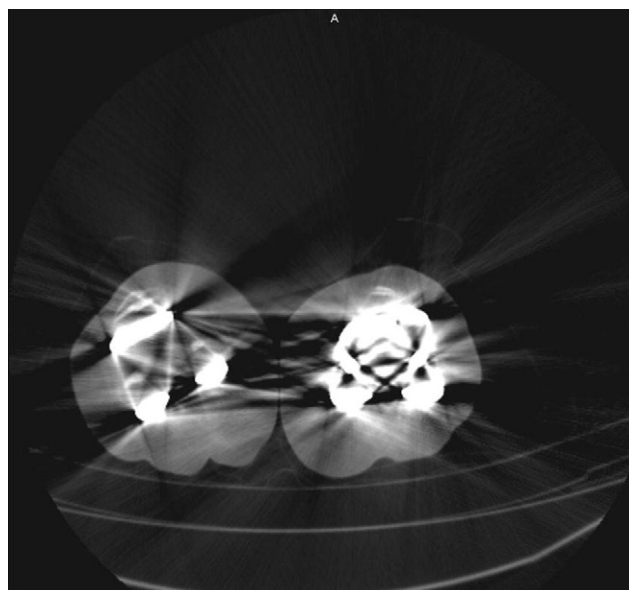


FIG 1. Example—metal artifact due to bilateral knee prostheses. kVp, 120; mA, 400; ms, 500; mAs, 200; thickness, 1 mm.

and screws. One phantom was constructed using titanium hardware; the other was constructed using stainless steel. Imaging was performed on a 64-row detector CT scanner (Aquillion 64; Toshiba America Medical Systems, Tustin, CA). Intrinsic factors contributing to hardware artifact were investigated by imaging both types of hardware, keeping imaging parameters constant. The effect of user-determined technical factors on artifact were examined by imaging the stainless steel phantom and varying, respectively, kVp, mAs, position of phantom within the scanner, reconstruction algorithm, acquisition thickness, reconstruction thickness, alignment of multiplanar reformat displays, image reconstruction method, and post-processing filter.

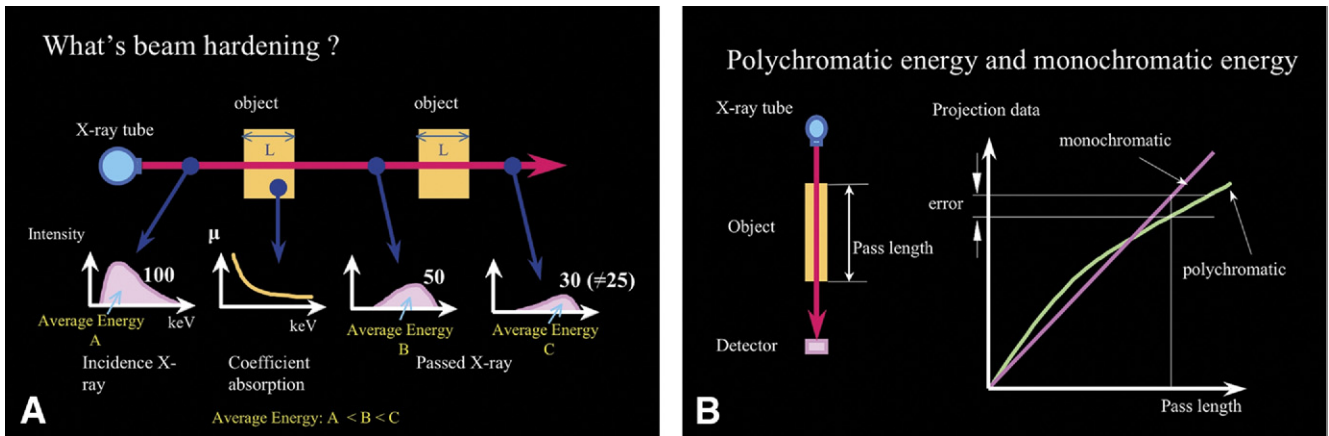


FIG 2. Physics of metal artifacts: (A) CT uses a polychromatic X-ray beam. As the polychromatic beam passes through an object, the effective energy is shifted toward higher values; thus, the beam progressively becomes “harder” as it traverses the object. For a given material, the mass attenuation coefficient varies according to the hardness of the incident beam. Materials, such as metal, with a higher mass attenuation coefficient result in significantly more pronounced beam hardening. The calculated CT number is therefore technically “in error” and results in beam hardening artifact (B). Beam hardening causes an error in the data received at the detector as shown. The projected data value of the monochromatic beam is proportional to its pass length. By contrast, the polychromatic beam results in a smaller value compared to the result expected for a monochromatic beam. This differential—an error in the projected data value—causes artifacts in the final image. The degree of error—and the resultant artifact—depends on the mass attenuation coefficient and the thickness (the pass length) of the object. (Color version of figure is available online.)

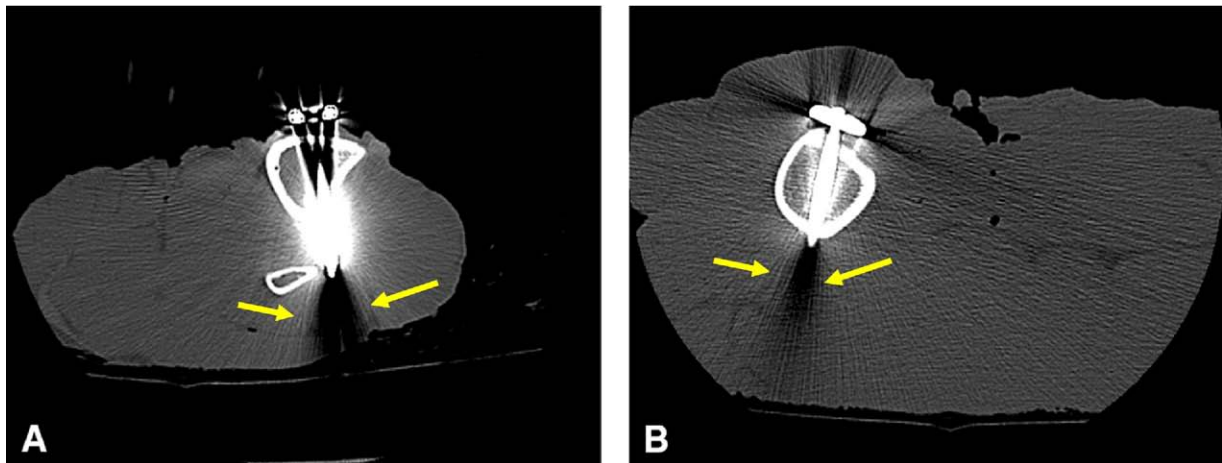


FIG 3. Artifact is worse with stainless steel (A) than with titanium (B). (Color version of figure is available online.)

Factors Affecting Metal Artifact—Intrinsic Factors

Type of Metal

Artifact is worse with stainless steel (Fig 3A) than with titanium (Fig 3B) because steel has a higher mass attenuation coefficient than titanium. Among metals currently used for orthopedic hardware and other surgical implants, titanium causes the least amount of artifact on CT images.¹ Less attenuating hardware material generates less missing projection data and therefore causes fewer artifacts.⁶

Shape/Geometry of Metal

The number of interfaces between an X-ray beam and a piece of metal can also influence the amount of artifact produced. More artifact can be expected with more complex shapes or greater numbers of hardware parts. In Fig 4A, the shape of the nail is symmetric in cross section, the attenuation of the x-ray beam is relatively uniform, and the artifacts become more pronounced in one direction. In Fig 4B, multiple screws in same cross section create more interfaces and the artifacts are dispersed across the entire image.

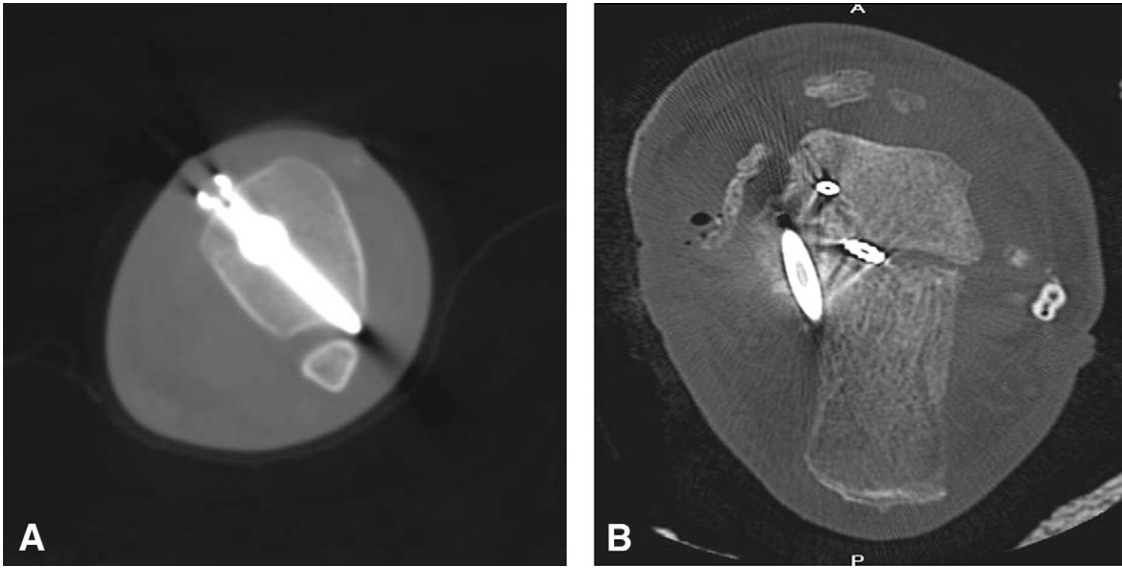


FIG 4. The number of interfaces between an X-ray beam and a piece of metal can also influence the artifact produced. More artifact can be expected with more complex shapes or greater numbers of hardware parts (e.g., plate and screws). (A) A single screw is simple in shape, so there is a relatively simple interface with the beam and more uniform attenuation and the artifacts are more pronounced in one direction. (B) Multiple screws in one cross section create more interfaces and the artifacts are dispersed across the entire image.



FIG 5. Increased kVp. CT images of a phantom scanned with 120 kVp (A) and 135 kVp (B), with all other factors remaining the same. These images demonstrate a very subtle improvement in the artifact using higher kVp. (Our scanner calibration does not allow for testing of other kVp values.) In a clinical setting, kVp must be balanced against dose considerations. (A) 120 kVp, (B) 135 kVp.

Factors Affecting Metal Artifact—Technical Factors

kVp

Contrast in an image depends on the difference in mass attenuation coefficients between different substances. Raising kVp results in smaller differentials among mass attenuation coefficients and thus lower

contrast in the image. Increasing the X-ray tube potential (kVp) will increase penetration of the X-ray beam through metal⁴ and theoretically can reduce the metal artifact. However, use of a higher kVp results in lower contrast in the image, because the differential of mass attenuation coefficients that causes the objects to become visible becomes smaller. Lowering image contrast using higher kVp has the effect of dampening

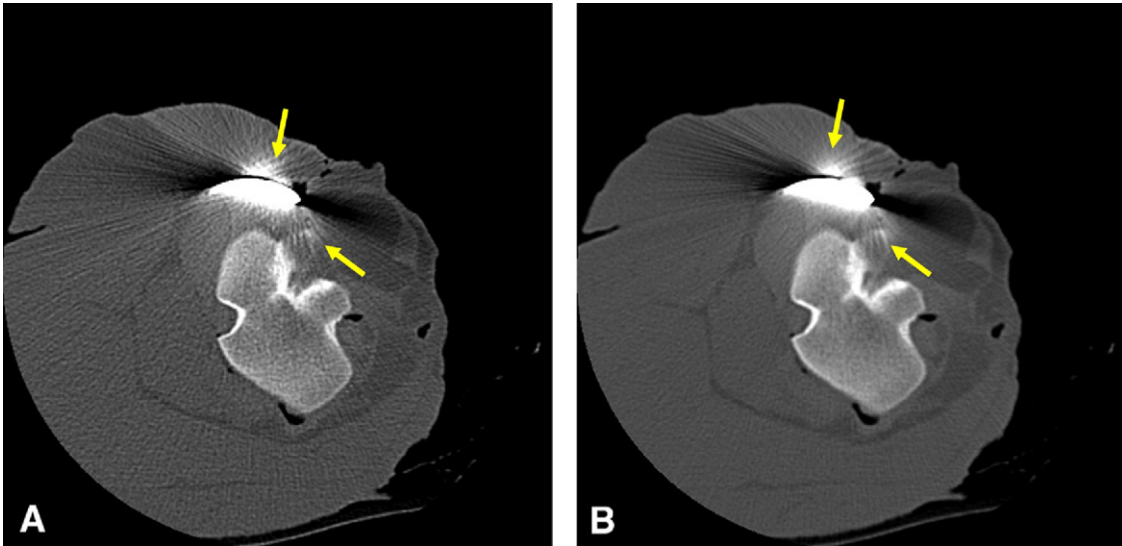


FIG 6. Increased mA. CT images of a phantom scanned with 100 mA (A) and 500 mA (B), with all other factors remaining the same. Note diminished artifact obtained with higher mA technique. (Color version of figure is available online.)

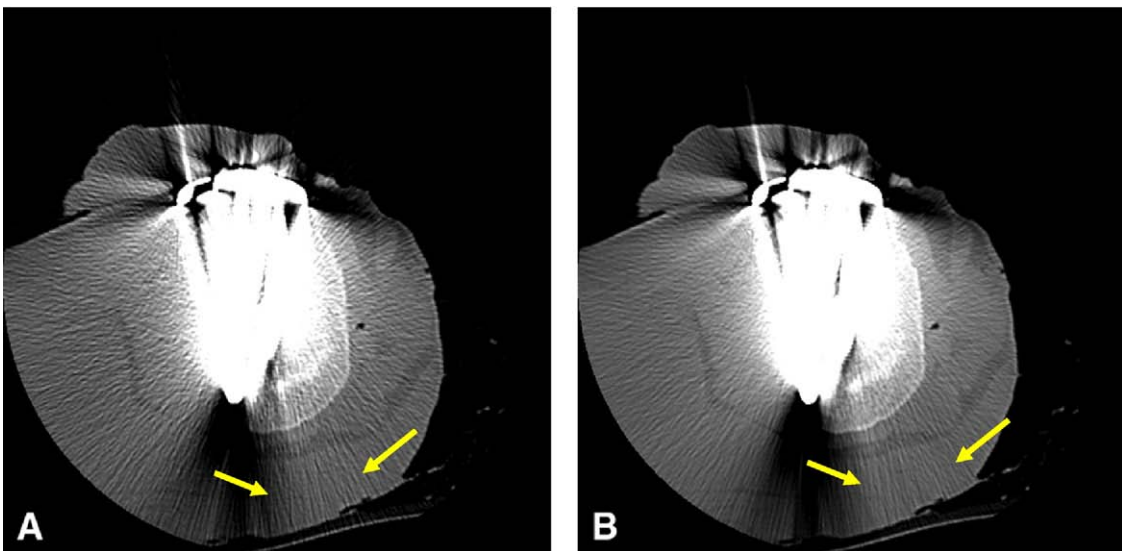


FIG 7. Scan rotation (exposure) time. CT images of a phantom scanned with exposure times of 500 mseconds (A) and 1500 mseconds (B), with all other factors remaining the same. Note diminished artifact obtained with longer scan rotation time. (Color version of figure is available online.)

the normally great differences in mass attenuation coefficients between metal and tissue, thereby reducing artifact (Fig 5). Of note, some authors do not find additional value in using exposures greater than 120 kVp.⁷ It is also important to note that increasing kVp will have the effect of increasing radiation dose to the patient.

mAs

Higher mAs result in more photons detected. When more photons are detected, there is less noise in the image and, therefore, metallic artifacts are decreased (Figs 6 and 7). As with kVp, it should be noted that use of higher mAs results in higher radiation dose to the patient.

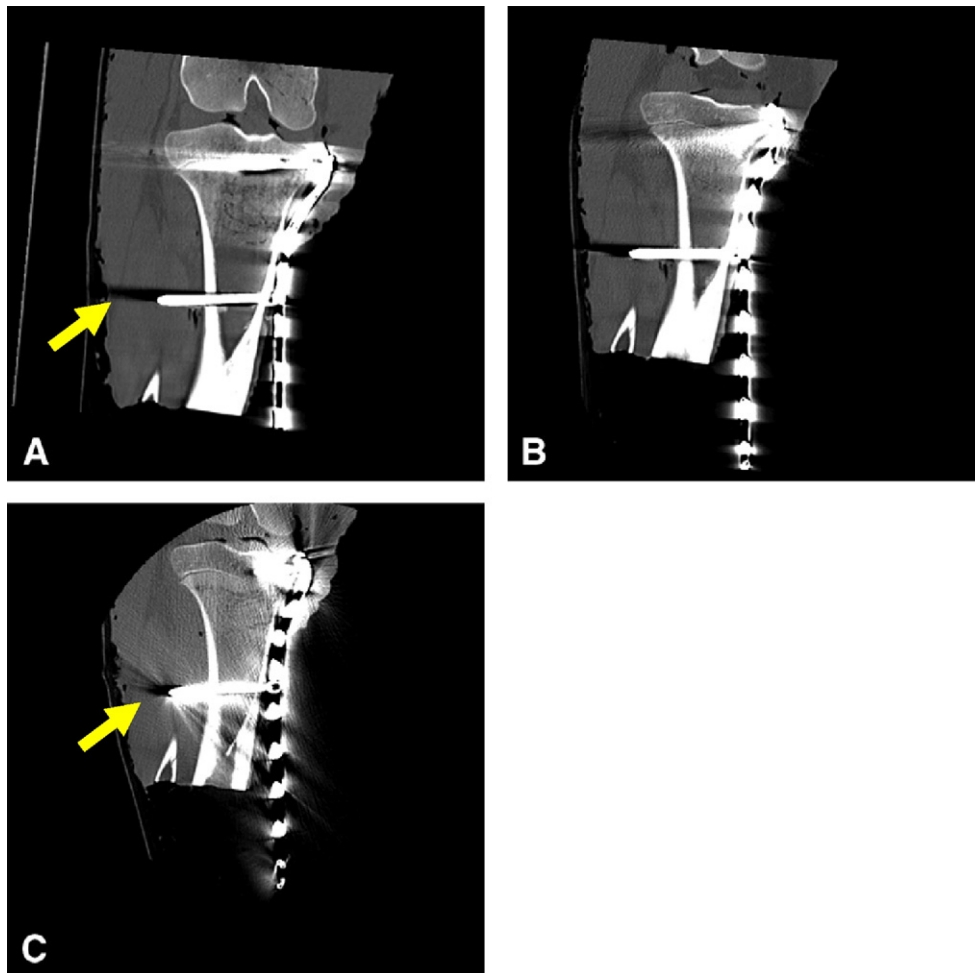


FIG 8. Positioning. The same phantom was scanned at different angles in relation to the scanner gantry, and coronal reformats were performed (approximating same coronal "slice"). Phantom aligned parallel to long axis of scanner (A), phantom rotated 45° to long axis (B), and phantom at 90° (C). Note that the orientation of the artifact with respect to the bone varies as the phantom position within the scanner is rotated. (Color version of figure is available online.)

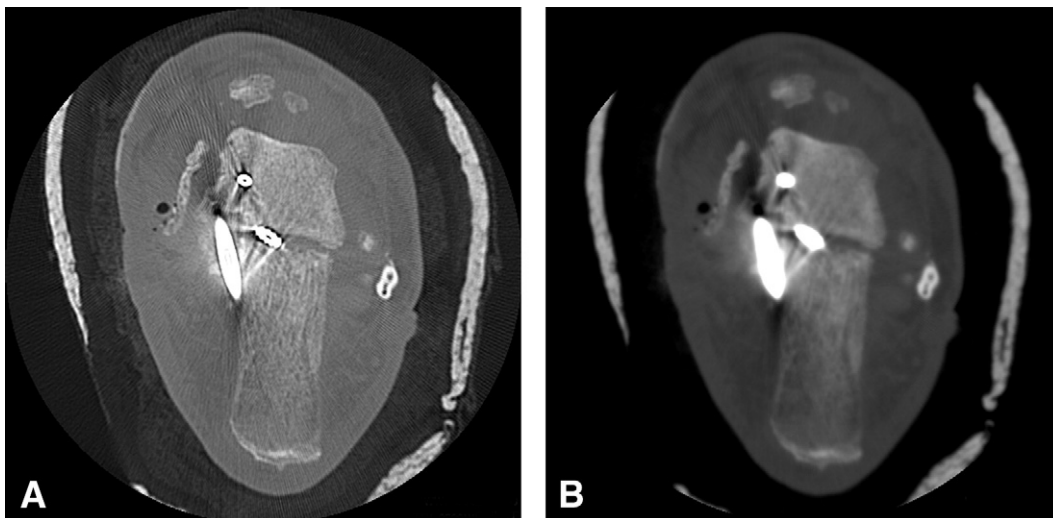


FIG 9. Reconstruction algorithm. Noncontrast CT scan of the ankle in a patient with Charcot arthropathy and osteoarthritis status post triple arthrodesis and medial column fusion. kVp, 135; mA, 350; ms, 500; Thk, 0.5 mm. Images were reconstructed in both bone (A) and soft-tissue (B) algorithms. Note that although bone detail is degraded, the hardware artifact is improved using the soft-tissue algorithm reconstruction.

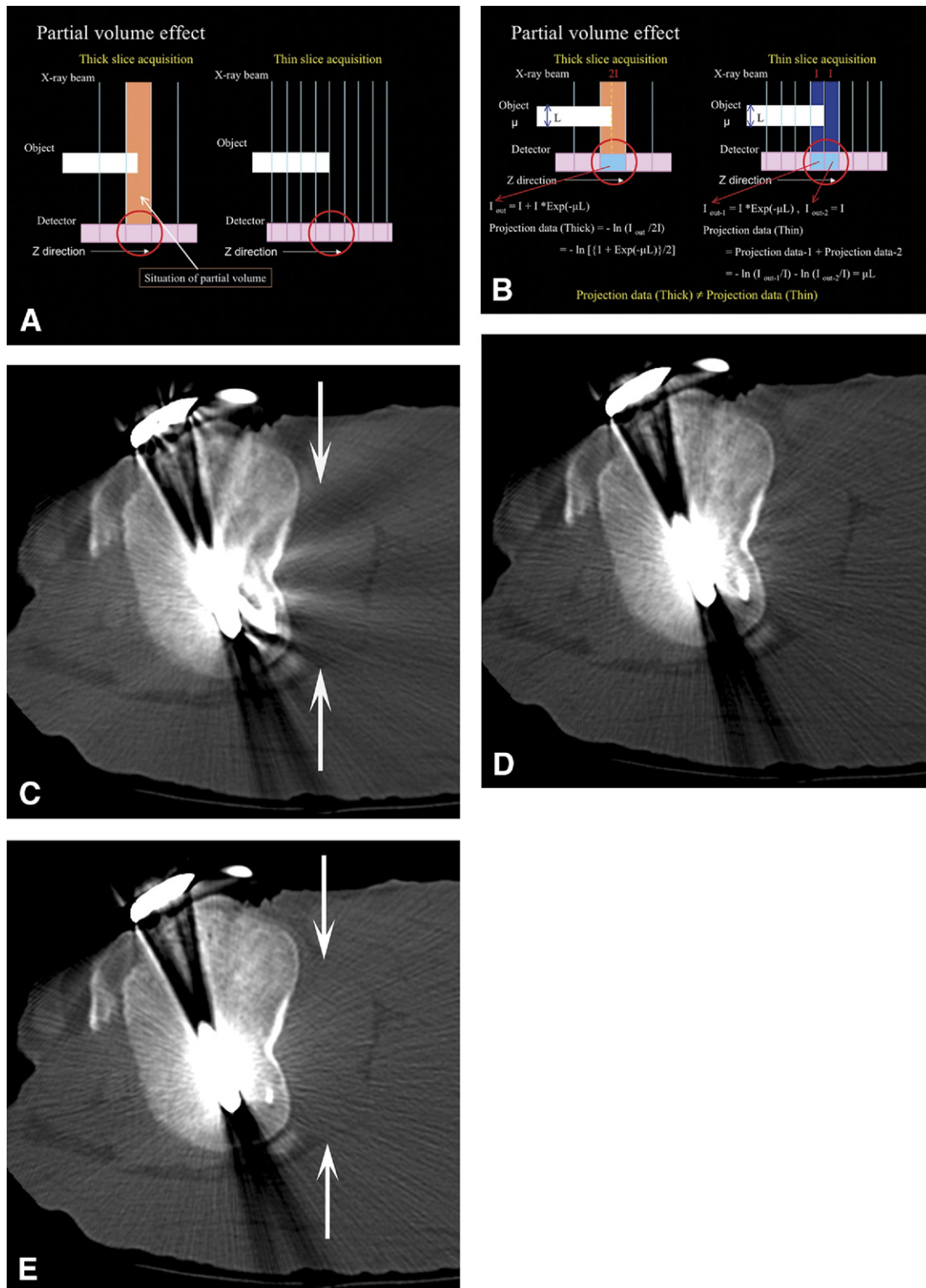


FIG 10. Acquisition thickness. The difference in the projection data between thick and thin slice acquisition causes partial volume artifact (A). In the back projection image reconstruction, the output from the detector is amplified by being processed through a "log-amplifier." For thick slice acquisition, the projected data value " $-\ln\{[1 + \exp(-\mu L)]/2\}$ " is not correctly projected as in the thin-slice acquisition; the projected data value is " μL " (the best possible situation is shown here) (B). Here, CT images of the phantom were acquired with (C) 2.0 mm \times 16 detectors, (D) 1.0 mm \times 32 detectors, and (E) 0.5 mm \times 64 detectors, with all other factors remaining the same. Note the decrease in artifact in (E) vs (C) due to thinner section acquisition. (Color version of figure is available online.)

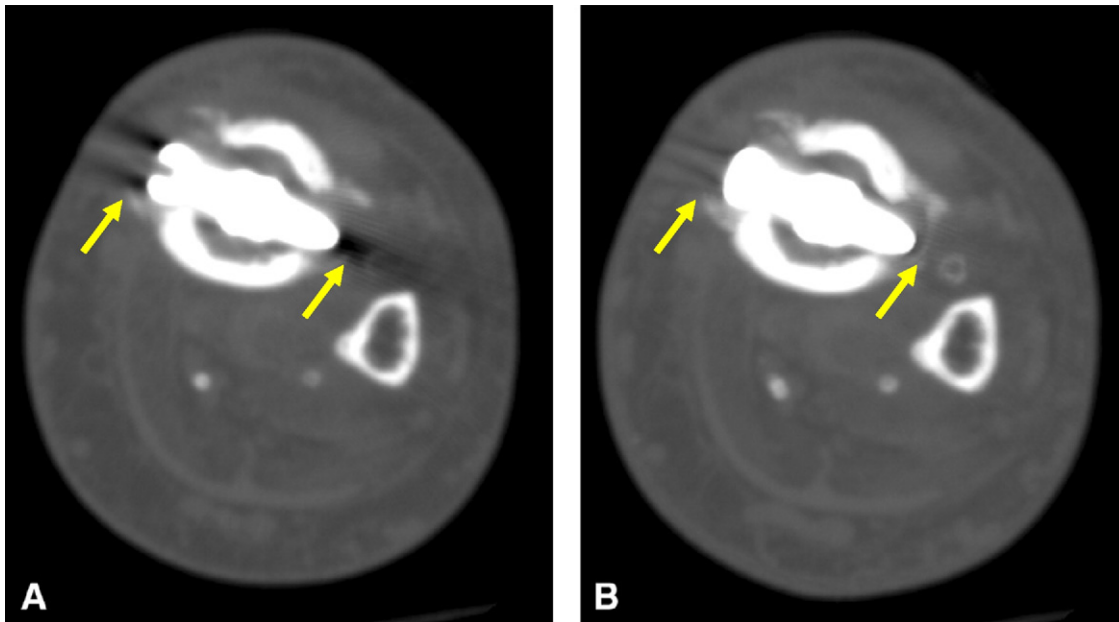


FIG 11. Reconstruction thickness. Left tibial fracture status post ORIF with intramedullary rod and interlocking screw. Noncontrast axial MIP reformations in 0.5 mm (A) and 5 mm (B) thickness are shown. Artifact is diminished with increasing thickness of the MIP reconstruction. kVp, 135; mA, 350; ms, 500; Thk, 0.5 mm. (Color version of figure is available online.)

Positioning

Artifact from metal will vary as the hardware orientation within the scanner is varied. Change in position of the hardware within the scanner may vary the number of interfaces between an X-ray beam and the metal, thus altering the resultant artifact. For example, the orientation of metal artifact with respect to an area of interest in the body may change if the body part is rotated within the scanner (Fig 8). If possible, the body part should be positioned so the X-ray beam traverses the minimum cross-sectional length of the metal (ie, the long axis of the metal should be placed perpendicular to the plane of the gantry).

Reconstruction Algorithm

Bone algorithm is generally preferred for display of fine bone detail, when no hardware is present, because of its edge-enhancing effect. However, edge-enhancement algorithms can exacerbate the appearance of metal artifact.⁴ Soft-tissue algorithms, which are not designed to promote edge enhancement, can help to minimize hardware artifact⁴ (Fig 9).

Acquisition Thickness

In general, thin-section acquisitions help to minimize artifact by reducing partial volume averaging.⁸

MDCT aids in reducing artifact by allowing acquisition of very thin individual sections (eg, 0.5 mm) (Fig 10). Although thinner sections can be degraded by increased noise, in this instance, the advantage of decreased partial volume artifact generally predominates.⁹

Reconstruction Thickness

Use of thicker reconstruction, here performed together with MIP technique, helps to minimize the effect of artifacts by better averaging of the signal within the voxel and by increasing the available signal-to-noise ratio (Fig 11). By contrast, too thick reconstructions increase blurring in the image, and image details can be lost.

Multiplanar Reformat Displays

Artifact generated from interaction between the X-ray beam and hardware has a 3-dimensional (3D) "shape." Artifact will therefore be worse in some image orientations and better in others. Reformats along certain planes can help to minimize interference from the artifact over the area of interest (Fig 12).

Image Reconstruction Method

Use of specific image reconstruction techniques can affect the severity of metal artifact. While MDCT can



FIG 12. Multiplanar reformat displays. Acquired axial image (A) shows artifacts extending 360° around the ankle. Sagittal (B) and coronal (C) reformats show artifacts restricted primarily to 1 direction. The sagittal plane corresponds to the dotted line; coronal corresponds to the solid line in (A).

help minimize artifact (specifically, by allowing acquisition of very thin sections), its wide area coverage can introduce a new kind of artifact. As the z-axis coverage gets wider with an increasing number of slices, cone beam artifacts can be introduced. The cone beam effect results in the displacement and misregistration of anatomy at the borders of high-density and low-density objects and can obscure important details¹⁰ (Fig 13). The effect is worse proportional to the increasing cone angle. Artifacts are often more pronounced for the data collected by outer detector rows than inner detector rows.⁸ This cone beam effect can worsen existing metal artifacts. A modified Feldkamp-

based cone beam reconstruction algorithm, in this instance, a proprietary technique called True Cone Beam Tomography (Toshiba Medical Systems) is used to compensate for cone beam artifacts from MDCT. Use of 3D back projection in helical scanning (as in the Feldkamp method¹¹) can help compensate for the divergence of the X-ray beam, consequently minimizing the cone beam artifact (Fig 14).

Postprocessing Image Filters

Metal artifact results in areas of raw data with low photon count. Fewer photons can traverse metal,

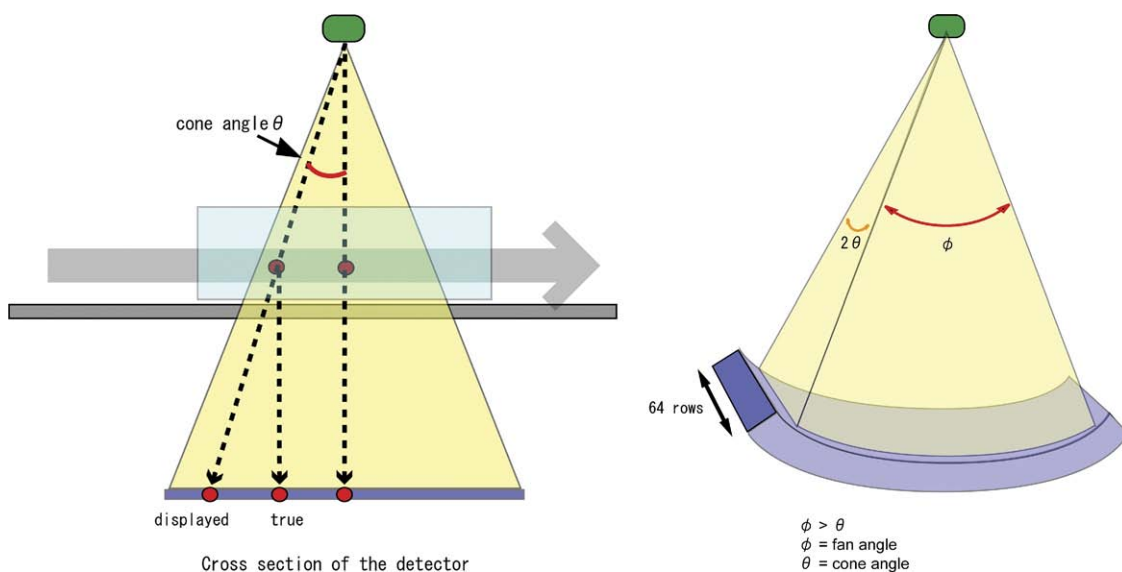


FIG 13. The cone angle (θ) refers to the divergence of the radiation beam along the z-axis. The detector fan angle is represented by ϕ . Objects that are imaged with the central rays of the beam are correctly registered, while objects that are traversed and imaged with divergent rays, especially distant from the central imaging plane, are misregistered away from their true position, i.e. the cone beam effect, resulting in a form of misregistration artifact. The cone beam effect is more apparent with data acquired at the outer rows. Thus, the artifact is more pronounced for structures that are distant from the central rows of the detector. The effect is also more pronounced when structures are off-axis in the body because, unlike a central object, an off-axis object is detected by different detector rows, at different degrees of beam angulation. (Color version of figure is available online.)

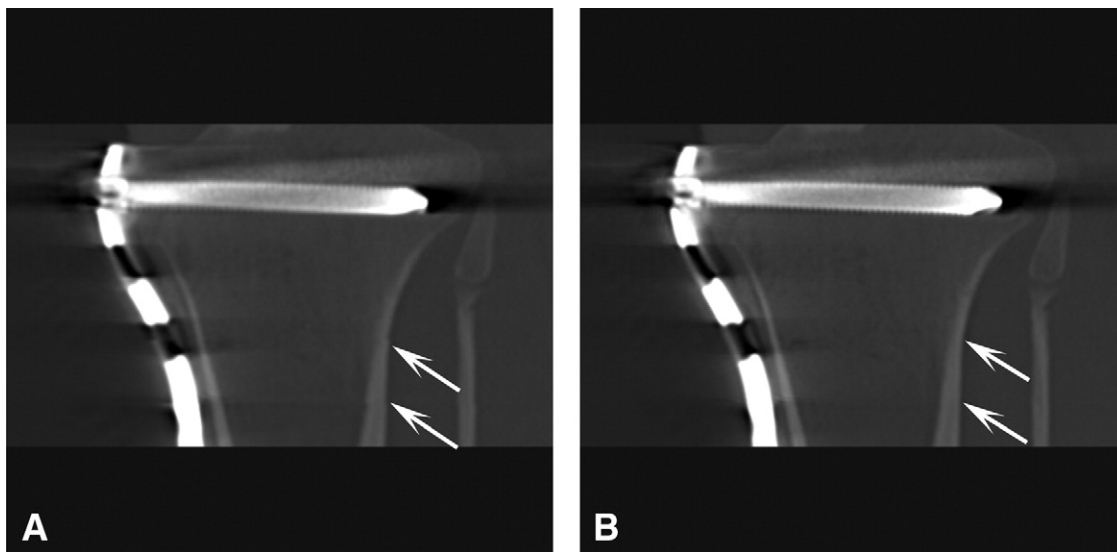


FIG 14. Image reconstruction method. CT images of phantom reconstructed without (A) and with (B) correction for cone beam artifacts (TCOT; Toshiba Medical Systems, Tustin, CA). Note the decreased distortion of the cortex once the reconstruction technique is applied.

because of its higher attenuation. This results in areas of raw data with a lower photon count, which, in turn, contribute to the effect that is perceived as metal artifact. Postprocessing image filters can help to correct raw data in areas of low photon count. In this

example, a proprietary adaptive raw data filter that works in all 3 spatial dimensions (in this instance, Boost 3D, Toshiba Medical Systems) identifies portions of the raw projection data where there is a disproportionate loss in X-ray signal and applies a

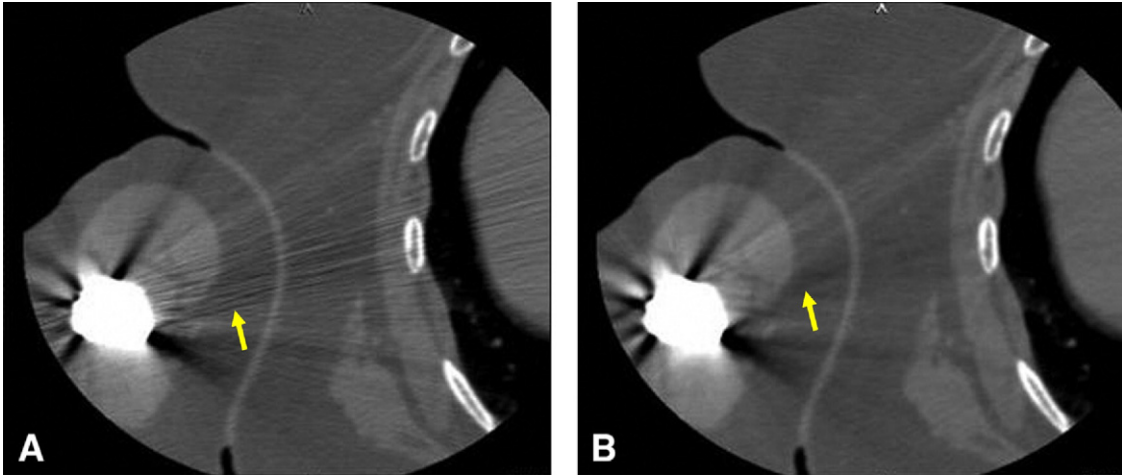


FIG 15. Postprocessing filter. CT images of patient with humeral hardware without (A) and with (B) postprocessing filter (BOOST; Toshiba Medical Systems). Note decreased conspicuity of artifact once the filter is applied. (Color version of figure is available online.)

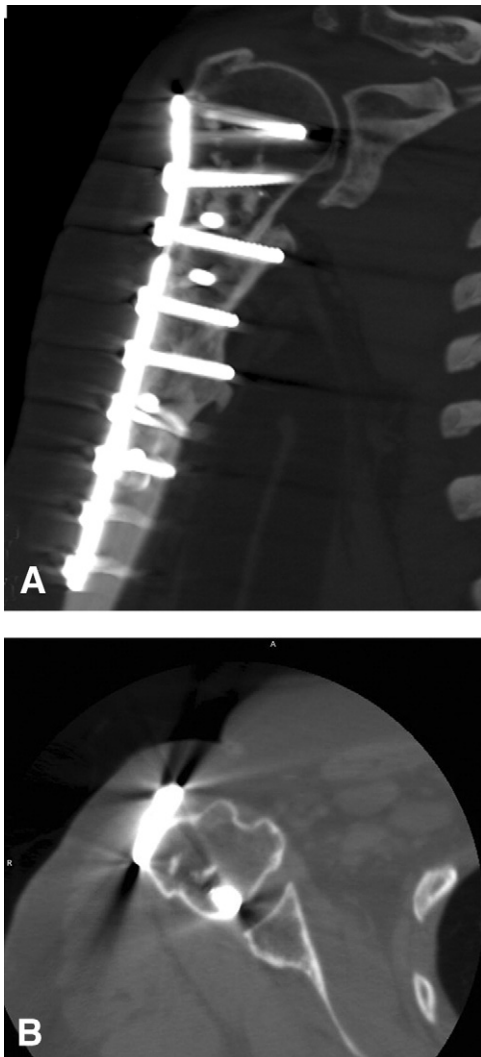


FIG 16. Shoulder pain status post ORIF of fracture. Coronal reconstruction (A) and axial acquisitions CT images (B). Acquisition

local 3D filter with smoothing effect to reduce image noise and streak artifacts. In areas of normal signal, no correction is applied and native image quality is preserved (Mather R, personal communication). Note that the use of such a filter can also result in subtle blurring of the image (Fig 15).

Sample Cases

Clinically relevant images combining all the factors mentioned above are shown in Figures 16-18.

Conclusions

Several conventional strategies are available for minimizing artifact from metallic hardware: use of higher kVp, higher mAs, patient positioning, and soft-tissue reconstruction algorithm. In addition, MDCT provides new opportunities for addressing artifacts from metallic hardware, including use of thinner section (0.5 mm) acquisitions; thicker reconstructions and multiplanar reformat technique; and choice of multiplanar reformat plane. Certain image reconstruction or filtering

parameters: kVp, 135; mA, 440; ms, 1000; mAs, 440; thickness, 0.5 mm. Despite the presence of a large amount of metal and considerable artifact, the position of metal in relation to the bones can still be evaluated, and the quality of cortical and medullary bone, as well as surrounding soft tissue anatomy, can be assessed.

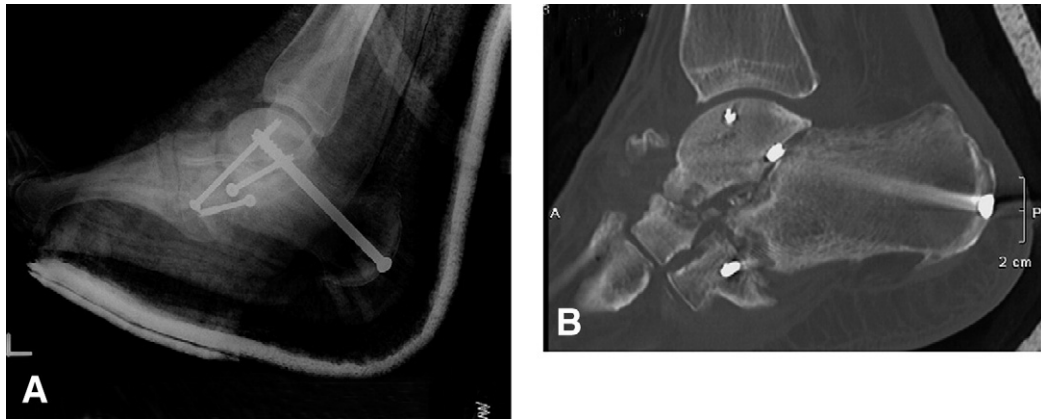


FIG 17. Radiographs of the ankle in a patient with Charcot arthropathy and osteoarthritis status post triple arthrodesis and medial column fusion (A). Absence of fusion is well-depicted despite the presence of hardware in the CT images (B). Acquisition parameters: kVp, 135; mA, 350; ms, 500; mAs, 175; thickness, 0.5 mm.

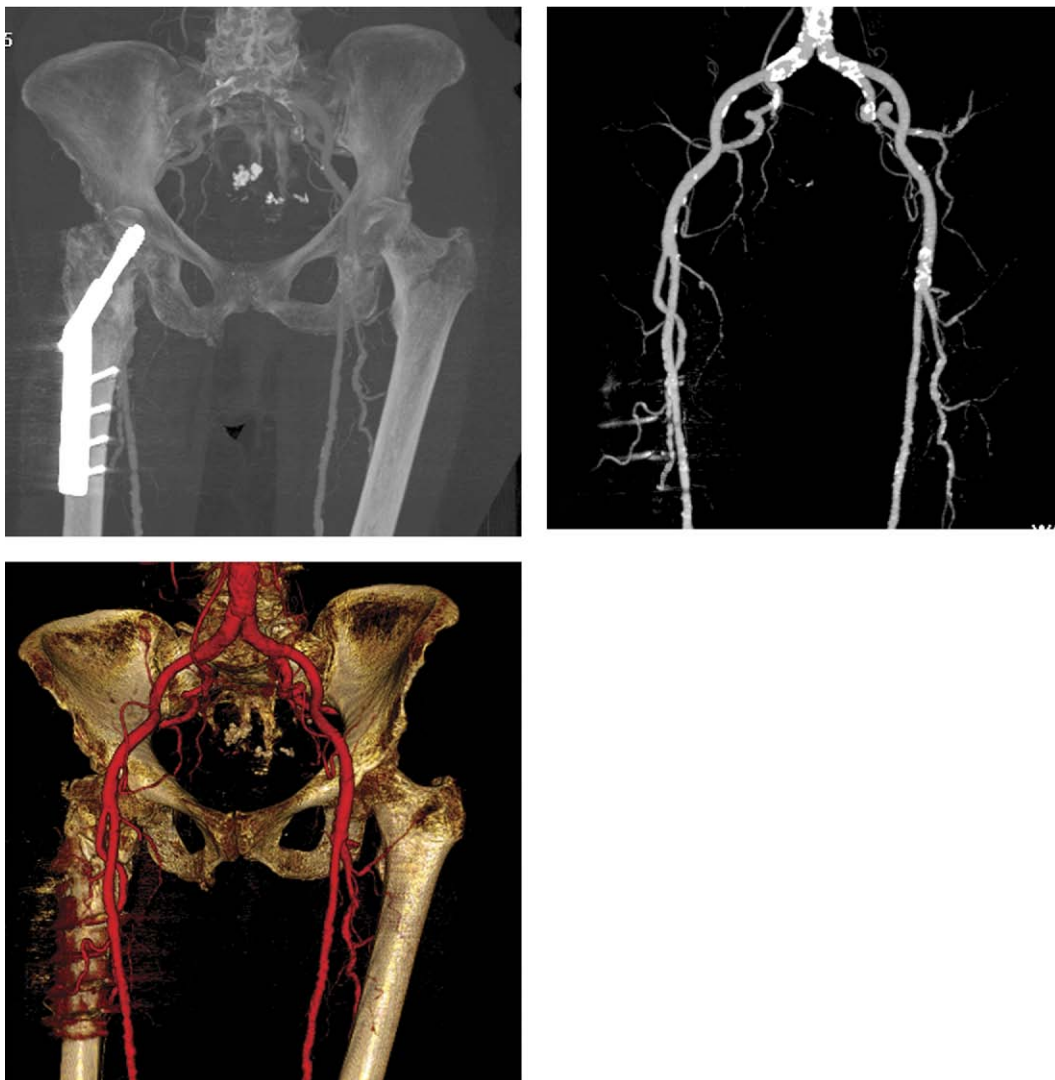


FIG 18. Ninety-year-old female with claudication and suspected ischemia. Despite the presence of a dynamic compression screw in her femur, the CT angiography with 3D volume rendering reconstruction was diagnostic and successfully demonstrated atherosclerosis without occlusion. Care must still be taken to avoid mistaking artifacts for pathology. Acquisition parameters: kVp, 120; mA, 400; ms, 500; thickness, 1 mm. (Color version of figure is available online.)

algorithms may also contribute to reduction of metallic artifacts.

Acknowledgments: The authors thank Yukihiro Ogawa for the schematic illustrations used in this article; Chloe Stevenson, Jeff Hall, and Steven Hopkins for assistance in data acquisition; Rich Mather for comments in physics; Carol Wilcox, Ann Cunha, Ron Kukla, and Hisashi Tachizaki for help in preparation of this project; and Clotell Forde and Giulia Zamboni for support and assistance in completion of this article.

REFERENCES

1. Vande BB, Malghem J, Maldague B, et al. Multi-detector CT imaging in the postoperative orthopedic patient with metal hardware. *Eur J Radiol* 2006;60:470-9.
2. Ohashi K, El-Khoury GY, Bennett DL, et al. Orthopedic hardware complications diagnosed with multi-detector row CT. *Radiology* 2005;237:570-7.
3. Buckwalter KA, Parr JA, Choplin RH, et al. Multichannel CT imaging of orthopedic hardware and implants. *Semin Musculoskelet Radiol* 2006;10:86-97.
4. White LM, Buckwalter KA. Technical considerations: CT and MR imaging in the postoperative orthopedic patient. *Semin Musculoskelet Radiol* 2002;6:5-17.
5. Hsieh J. Image artefacts, in CT. In: Goldman LW FJ, editor. *Syllabus: A Categorical Course in Diagnostic Radiology Physics: CT and US Cross-Sectional Imaging*. Oak Brook, IL: Radiological Society of North America, 2000. p. 97-115.
6. Robertson DD, Weiss PJ, Fishman EK, et al. Evaluation of CT techniques for reducing artifacts in the presence of metallic orthopedic implants. *J Comput Assist Tomogr* 1988;12:236-41.
7. Haramati N, Staron RB, Mazel-Sperling K, et al. CT scans through metal scanning technique versus hardware composition. *Comput Med Imaging Graph* 1994;18:429-34.
8. Barrett JF, Keat N. Artifacts in CT: Recognition and avoidance. *Radiographics* 2004;24:1679-91.
9. Hsieh J. *Computed Tomography: Principles, Design, Artifacts, and Recent Advances*. Bellingham, WA: SPIE, The International Society for Optical Engineering, 2003.
10. Nagel HD. Multislice CT technology. In: <http://www.multislice-ct.com>. Accessed 2004.
11. Feldkamp LA, Davis LC, Kress JW. Practical cone-beam algorithms. *J Opt Soc Am* 1984;6:612-9.